ISBN: 978-3-95450-262-2 ISSN: 2673-5350 doi: 10.18429/JACoW-IBIC2025-TUBC01

ISOLATING THE LIGHT OF A SINGLE BUNCH: DETERMINING THE VIABILITY OF OPERATING VERTICAL-PLANE PULSE PICKING BY RESONANT EXCITATION AT DIAMOND-II TO SERVE TIMING MODE USERS

S. Wilkes*, P. N. Burrows, John Adams Institute, Oxford, United Kingdom
L. Bobb, B. A. Coulson, G. Karras, A. F. D. Morgan, M. R. Warren
Diamond Light Source, Didcot, United Kingdom

Abstract

Pulse Picking by Resonant Excitation (PPRE) enables synchrotron facilities to provide single-bunch light for timing users without interrupting multi-bunch operation. We report the first vertical-plane PPRE tests at Diamond using the Multi-Bunch Feedback system, achieving vertical bunch-size growth and measurable X-ray enlargement. A simple novel optimisation improved PPRE purity by reducing the baseline emittance. Beyond readily-available diagnostics, we demonstrate how crystallographic diffraction can be used as a user-relevant method to characterise PPRE with statistically significant evidence of isolating a single excited bunch. Together, these methods provide a practical and user-orientated framework for synchrotron facilities considering similar timing-mode capabilities.

INTRODUCTION

Whilst most scientific users of a synchrotron facility require maximal brilliance, the "flux users", some scientific users instead prioritise temporal resolution – the "timing users". Example experiments may include pump-probe measurements [1], or studying the dynamics of a chemical process [2]. Diamond currently offers timing users a hybrid fill-pattern, which ensures the target X-ray pulse has an unlit gap either side of it [3]. For Diamond-II, there are additional constraints on fill patterns, beam lifetime, and instability thresholds [4] that may result in the hybrid fill not being offered. A back-up approach is sought.

PPRE is a method, first developed at BESSY, to simultaneously cater to timing users and regular ('flux') users [5]. Conceptually, PPRE works by isolating the light from a single bunch, such that the beamline effectively only sees a single bunch (thus X-ray pulse) in the ring. The two key ingredients for PPRE are the deliberate increase in the size of the X-ray beam and the amount by which the unwanted bunch light is blocked by the beamline optical-apertures. The unwanted bunches are known as the 'train'; for PPRE, any light from the train that reaches the experimental area constitutes background. A schematic of PPRE is shown in Fig. 1. To increase the vertical X-ray beam size requires to first increase the electron bunch size. At Diamond this can be done with the Multi-Bunch Feedback (MBF) system (for details, see [6]). Owing to its flexibility, users would have the option to select arbitrary bunches to excite, allowing for experiment-tailored X-ray pulse structures.

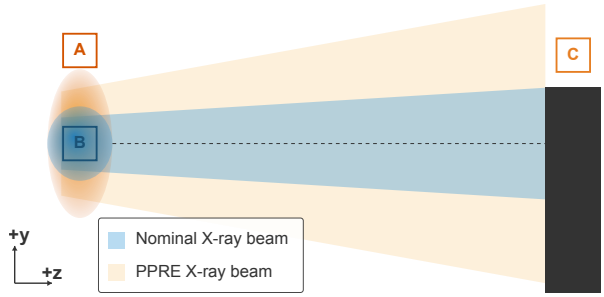

Figure 1: A schematic of the vertical PPRE procedure. As each bunch emits synchrotron radiation, the optical apertures at the beamline (C) must be positioned such that the light from the train (B) is blocked, whilst ensuring that the light from the excited electron bunch (A) is able to pass through.

Some samples used in timing experiments can degrade if exposed to continuous levels of synchrotron radiation, thus requiring illumination from only a single X-ray pulse. Due to blocking of the background radiation, PPRE degrades samples used by timing users more slowly than hybrid-fill. The main trade-off for PPRE is that the amount of flux delivered to the timing user is at least a couple of orders of magnitude smaller than a pure single bunch [5]. Whilst these conditions are sufficient for a subset of timing users, some other timing users may still prefer to seek out other options. Nonetheless, the clear advantage of methods like PPRE is that flux users are unaffected [5, 7].

This paper reports on investigations at Diamond on how to offer PPRE in the vertical plane as an alternative to hybrid fill for Diamond-II. In particular, we highlight both the methods for driving PPRE and its practical assessment at a beamline for its suitability to serve timing users.

EXPERIMENT SET UP

The storage ring was set up for user-beam operation: 900 bunch train (300 mA) and fast-orbit feedback on. In addition to bunch-by-bunch feedback, the MBF system served a dual role: utilising its excitation capability to increase the equilibrium vertical size of each selected bunch. This approach is similar to [8]. The MBF kick power is specified in decibels, but for simplicity we report its amplitude. The conversion, which takes kicks from a logarithmic to a linear scale, is

* juan.martinezwilkes@physics.ox.ac.uk

ISBN: 978-3-95450-262-2 ISSN: 2673-5350 doi: 10.18429/JACoW-IBIC2025-TUBC01

given by

$$\text{amplitude} = \exp\left(1/20 \times \text{decibels}\right). \quad (1)$$

Emittance is calculated from two X-ray pinhole cameras located after dipole bends in the storage ring [9] which both capture the electron beam size. Note, due to the camera exposure (50 ms) being much greater than the revolution time 1.86 µs, it is only experimentally valid to take emittance measurements when the all the bunches are being driven by the MBF. As the emittance growth of each bunch driven by the MBF is independent of the emittance of other bunches, this still provides a reliable proxy.

The I19 crystallography beamline, which operates X-rays in the range 5–25 keV [10], must retain the capability to host timing user experiments for Diamond-II. Thus, it acted as a representative platform for testing PPRE. The photon beam properties at I19 were first quantified with a diagnostic camera (its set-up consists of a scintillator screen, lens and a camera), located immediately after the Double Crystal Monochromator (DCM). This approach required no prior set-up but, like before, is only valid when all bunches are driven due to the camera's exposure time.

A second diagnostic method was to place a Hamamatsu photodiode (S3584-09) at the beam-stop to monitor flux at the sample-point. A photodiode is a semi-conductor based device that produces a voltage when exposed to light. They can be used for accurately determining both the relative amount of flux (based on voltage reading) and absolute amount (once the voltages have been calibrated to photon count). Photodiodes of this type and calibre are a standard piece of equipment at beamlines; they are easy for staff to set up, and provide the fastest way to gauge the flux that would reach a sample. Although less advanced in terms of temporal resolution compared to the avalanche diode described in [5], these photodiodes are a comparatively cheaper and more accessible sensor.

To detect the flux of just a single bunch required more advanced instrumentation. A further constraint was that any measurement also had to be interpretable to potential timing users. Hence, a diffraction measurement of a crystal using PPRE was undertaken.

Lastly, a mechanism was required to block the synchrotron radiation emitted from the electron bunch train. For this we repositioned a moveable fixed-size aperture, of fixed size 9×6 mm (width $\times$ height), situated before the DCM, to block the X-rays emitted from the train whilst still allowing a proportion of the X-rays from the excited bunch to propagate along the beamline (see Fig. 2).

PPRE EXPERIMENT RESULTS AND ANALYSIS

Two distinct experimental campaigns were performed at the I19 beamline, each with different objectives and measurement approaches. The first experiment focused on establishing proof-of-principle feasibility for PPRE using the Multi-Bunch Feedback system, requiring only basic diagnostic measurements to determine whether vertically enlarged electron beams could be successfully generated and translated to enlarged X-ray beams. The second experiment involved more sophisticated instrumentation in the I19 user experimental area to quantify PPRE performance through methods that would be easily implementable by beamline staff and readily interpretable by potential timing users.

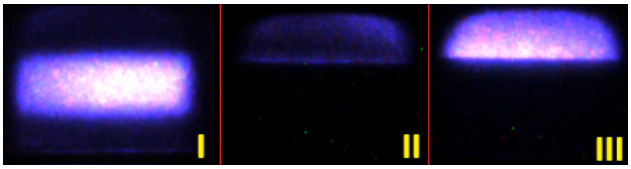

Figure 2: Experiment-I images from the I19 diagnostic camera. (I) Nominal X-ray beam. (II) After positioning movable window to block train light. (III) MBF driving all bunches at 0.8 kick amplitude, demonstrating PPRE operation. The camera exposure was increased from 0.4 to 1.5 s after (I).

Experiment-I: Measurements with the I19 Diagnostic Camera for PPRE Characterisation

This experimental phase utilised the main X-ray diagnostic camera on the I19 beamline. It allowed us to conduct our proof-of-principle experiments, such as determining the performance of using the Multi-Bunch Feedback system to enlarge electron bunches and thus the X-ray beam. We conducted a second complementary investigation, exploring a novel optimisation method to enhance PPRE purity without requiring additional kick strength.

Testing the Capability of the Multi-Bunch Feedback System for Driving the Electron Beam The fundamental observations are plotted in Fig. 3. The immediate first test we conducted was to look at the response curve of the vertical electron bunch size to MBF driving amplitudes (see Fig. 3(c)). We found that the maximum factor of vertical bunch-size growth was $\sim 17\times$, demonstrating the versatility of the MBF system.

The first sets of PPRE measurements comprised of driving all bunches of the electron beam with the I19 insertion device gaps and DCM adjusted for 25 keV photons and observing the X-ray beam size at the I19 diagnostic camera. For consistency between measurements, the gain and exposure of the camera were kept constant. The downside is that this risks not fully capturing the full extent of the beam as it becomes more diffuse. This means this camera-setting may underestimate the size of the excited beam since the size of the X-ray beam is recorded from the FWHM. The results are shown in Fig. 3(a). With these two measurements, one can then stitch them together to see how the vertical size of the X-ray curve changes with the vertical electron size – see Fig. 3(b). Note the β_y values are 2.3 m and 27.8 m for I19 and the pinhole respectively.

Although the electron bunch size was successfully increased, the corresponding X-ray beam size showed only

ISBN: 978-3-95450-262-2 ISSN: 2673-5350 doi: 10.18429/JACoW-IBIC2025-TUBC01

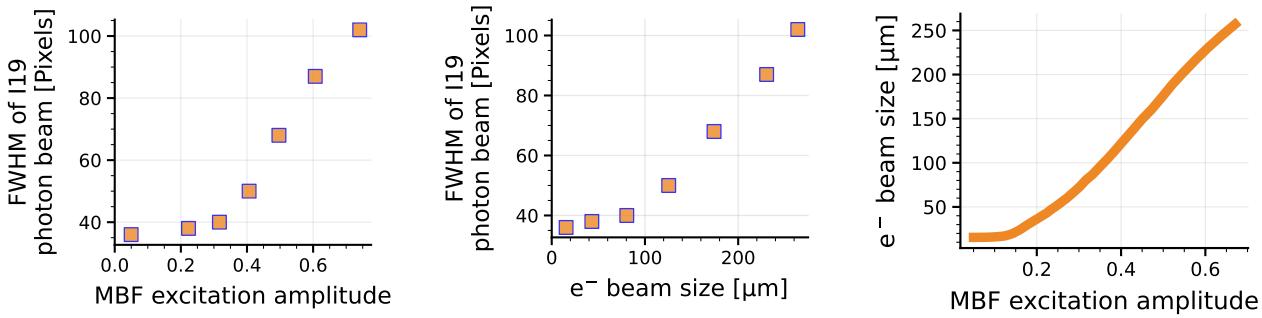

(a) Vertical FWHM (in pixels) of the X-ray beam as seen from the I19 diagnostic beamline camera against MBF driving amplitude.

(b) Our observed correspondence between vertical electron size at the pinhole camera and the vertical X-ray beam FWHM at I19.

(c) Vertical electron beam size, as measured from the pinhole cameras in the storage ring, with increasing MBF driving amplitude.

Figure 3: Measurements from Experiment-I showing vertical beam enlargement (both electron and X-ray) using the MBF. These measurements act as 'effective calibration curves' between the excited electron bunches and X-ray beams. There is a small initial plateau region before the linear increase in bunch and beam size with kick.

modest growth. Nevertheless, the observed fractional increase in X-ray beam size is still comparable with what has been offered at BESSY [5].

Novel Optimisation to PPRE We also tested a novel optimisation to improve the purity – the signal-to-background ratio of flux from the driven single bunch compared to the train. The idea is to enhance the relative bunch enlargement without increasing kick strength; since vertical dipole kicks add to existing emittance, reducing the baseline emittance increases the relative growth from excitation (for a numerical demonstration, see Fig. 1 in Ref. [11]).

We first conducted measurements under standard machine conditions. In order to move our experiment closer to real PPRE conditions, the moveable fixed-aperture window was moved into place (see Fig. 2). The I19 diagnostic camera exposure was increased to account for the lower flux, then kept fixed. Finally, various MBF kick amplitudes were tested on the electron beam, with performance quantified by summing the signal in the illuminated region (II and III of Fig. 2).

To test our optimisation hypothesis, we performed a LOCO procedure [12] to reduce the undriven vertical beam size. The vertical emittance was reduced from 8 pm · rad to 3.96 pm · rad. After repositioning the aperture appropriately, the experiment was repeated with the same range of MBF kick amplitudes for comparison with the baseline. To account for differing conditions (e.g. beam current), all readings were normalised to the undriven case (here representing the background). The results are shown in Fig. 4. When the MBF amplitude is zero ("OFF"), this corresponds to flux collected for the unperturbed beam, serving as the baseline for comparison. The higher the recorded ratio, the higher the 'purity' for beamline users, as this indicates better isolation of the excited bunch from the background train. The results indicate a clear performance gain: at higher amplitudes the squeezed case yields ~ 40 % more relative signal. Owing to the fixed aperture, however, enlarging the standard beam beyond ~ 0.3 amplitude does not further increase flux. In

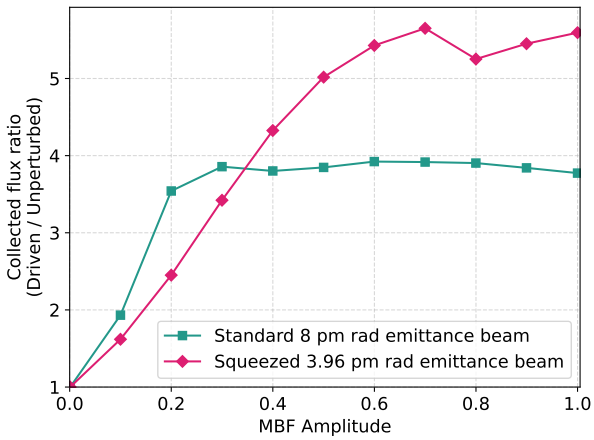

Figure 4: The increase in X-ray flux relative to PPRE-OFF as a function of MBF driving amplitude for standard and vertically squeezed electron beams.

fact, Fig. 4 suggests it may even reduce as the beam becomes increasingly diffuse (c.f. Fig. 3(c)). This suggests an optimal enlargement exists, but the MBF at Diamond is not a limiting factor in delivering PPRE.

Experiment-II: Preliminary Findings from the User Experimental Area at the I19 Beamline

Within this Subsection, we focus on more advanced instrumentation on the I19 beamline that we used to quantify our initial PPRE attempts. The methods were chosen to be straightforward for a beamline to implement and that clearly communicate to potential timing users either the utility or constraints of PPRE. Since these methods are based on taking readings around the sample-point at I19, more care was required on the set-up. As one can see in Fig. 2, moving the aperture upwards effectively alters the optical axis. As such, the beamline must be realigned. This took around 15 minutes to do, for instance by adjusting the DCM offset and

ISBN: 978-3-95450-262-2 ISSN: 2673-5350 doi: 10.18429/JACoW-IBIC2025-TUBC01

adjusting the focusing mirrors. It is, though, much easier to switch between PPRE-OFF and -ON once these alignment values have been established.

Photodiode at the Beamline Sample Backstop Like in the previous experiment, the aperture was adjusted to block the X-rays from the train. The beamline optics were then aligned so that the new effective X-ray source would reach the sample adequately. Then we tested two modes; first we recorded the background X-rays with the MBF driving off and secondly we recorded the X-ray levels with the MBF driving all bunches. The photodiode voltage output was recorded across 10 seconds readings taken every 100 ms. These voltage measurements correspond to the X-ray flux reaching the I19 beam-stop. The calculated voltage ratio between the two modes mirrors the measurements made in Experiment-I. The results can be found in Table 1. They show a more favourable ratio than what was recorded for the standard electron beam in Fig. 4, indicating improved measurement performance.

Table 1: Photodiode Voltage Measurements for the PPRE-OFF and -ON (MBF Set to 0.74 Amplitude) at I19 Beam-Stop

Condition	Voltage (V)
MBF driving OFF	0.14835 ± 0.00002
MBF driving ON	0.62050 ± 0.00008
Ratio of collected flux	4.18258 ± 0.00074

Diffraction Measurement of a Single Excited Bunch (PPRE) As I19 is a crystallography beamline, it is important that any quantification of PPRE should easily communicate its usefulness to potential I19 users by including a representative diffraction measurement from a well-known crystal. This approach effectively employs the beamline as a specialised photon detector for a tangible real-world scenario.

The crystal selected was the polymeric compound $[CuF_2H(pyz)_2]$ (PF_6), where 'pyz' stands for pyrazine. This is used regularly on I19 as a test system [13]. The beamline was configured for 18 keV photons (0.6889 Å). Rather than attempting a full crystallographic reconstruction, we focused on measuring individual diffraction peaks to compare intensities between PPRE-ON and -OFF states. The sample was placed in the I19 diffractometer and rotated in steps of 0.1° up to 0.5°, with photons counted using a PILATUS 2M detector.

To gather initial statistics, angular sweeps were repeated five times. As any test crystal can be used for this purpose, and each angular sweep took less than one minute, this demonstrates this approach is a quick and practical method for assessing realistic PPRE delivery.

To extract the additional signal from PPRE, we had to create a data-analysis pipeline. The first step was to identify the Bragg peaks from the background, as shown in Fig. 5.

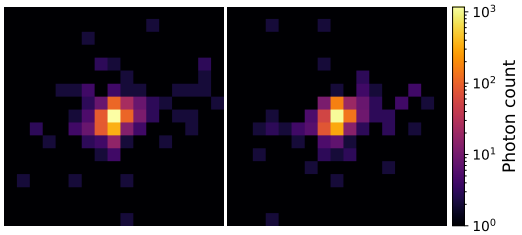

Figure 5: A persistent Bragg peak from Experiment-II; images are control conditions and PRRE-enabled respectively.

Since by inspection these peaks were sparse, we employed a simple local maxima routine; details are in the Appendix. The experimental objective centred on comparing diffraction peak intensities between PPRE-ON and PPRE-OFF states. To ensure robust comparison, for a peak to be counted in the final statistical analysis it had to satisfy three conditions simultaneously: (i) all peaks found must then persist between angular changes, (ii) peaks must persist between repeat readings, (iii) any peak in the PPRE-OFF measurement must also be found within PPRE-ON.

Once a peak was established, we had to find its intensity. The simplest method was to record the maximum of the peak, though this exposes the result to fluctuations. A more robust method is to fit a 2D-Gaussian to the peak and record its height. This allows us to take into consideration the surrounding pixels. In general, our data-analysis philosophy was to begin with simple or parameter free steps before building in any further complexity. We present the methods employed, in increasing order of sophistication, in Table 2.

Next we investigated mitigating systematic errors. For instance, to remove detector noise we devised a background subtraction routine. Details are in the Appendix. Once the background noise had been subtracted, the same routines as before could be used. Systematic errors that we did not address were for instance not accounting for the decay in the electron beam current between our measurements of PPRE-OFF and PPRE-ON (this systematic works against our favour). Future experiments should aim to take greater care in recording the ambient operating conditions, and, to improve statistical confidence, increase the number the repeat readings.

In all cases, the measurement data had to be averaged to produce a final peak-intensity ratio. Due to the high background rates (flux leakage originating from the train), multiple statistical approaches were considered (see Appendix for details). From this, we could determine the sigma-significance of our readings and present a meta-analysis to help validate our measurement robustness. If the null hypothesis was a non-detection of a single bunch, then with 6 out of 8 analyses approaches yielding z-scores ≥ 1.8 (corresponding to p-values $\leq 3.5\,\%$) we believe this validates the conclusion that we performed the first measurement of a vertically excited single bunch within the train.

To prevent damage to the sensor array, due to the high background levels, the X-ray transmission through the diffrac-

ISBN: 978-3-95450-262-2 ISSN: 2673-5350 doi: 10.18429/JACoW-IBIC2025-TUBC01

Table 2: Ratio of measured Bragg peak intensities for PPRE-enabled versus control from the I19 diffractometer. Due to high background levels, different statistical methods and peak fitting approaches were used. The values computed required increasing numbers of assumptions from upper-left to lower-right. Sigma significance values (in parentheses) are calculated relative to a ratio value of unity. The highlighting of red signifies $\sigma < 0$ and green $\sigma > 1$.

Method of error analysis	**Max of peak**	**Fitted 2D-Gaussian peak**	**Max of peak (Background Subtracted)**	**Fitted 2D-Gaussian peak (Background Subtracted)**
Standard quadrature (unweighted)	1.0166 ± 0.0063 (2.6σ)	0.9681 ± 0.0164 (-1.9σ)	1.0166 ± 0.0063 (2.6σ)	0.9918 ± 0.0126 (-0.6σ)
Standard quadrature (inverse-variance weighted)	1.0065 ± 0.0035 (1.8σ)	1.0062 ± 0.0033 (1.8σ)	1.0065 ± 0.0035 (1.8σ)	1.0061 ± 0.0033 (1.8σ)

tometer was set to 10 %. The set-up at the beamline must be optimised to bring down the background to practical levels. Given the large degree of transmission headroom, we remain confident that the method of using a diffractometer will retain the resolving power to characterise PPRE (even if exposure times are increased).

CONCLUSION

This paper presents the first experiments into the feasibility of vertical-plane PPRE and its challenges. This was achieved by taking measurements at a representative beamline, I19. This demonstrated the practicality of the measurement methodology in establishing the current operational performance and highlighting areas of improvement. With regards to providing timing mode users with PPRE at Diamond-II, future work must prioritise configuring the beamline to limit background X-ray flux leakage. Fortunately, on the machine side, the existing MBF system at Diamond proves highly capable for providing the controlled electron beam emittance enlargement required for PPRE.

As I19 expressed an interest in continuing to serve timing users at Diamond-II, this motivated us to perform diffraction measurements using PPRE. Despite challenging background conditions, we used a variety of statistical analyses to suggest that we detected the additional Bragg diffraction intensity from a single vertically excited electron bunch. Owing to the relevance of such a method to potential timing users, we therefore conclude that future campaigns to develop PPRE should employ diffraction measurements.

We have also shown that for early-stage preparation work, a standard beamline X-ray diagnostic camera can adequately determine the X-ray beam enlargement from a vertically excited electron beam, with further calibration possible using readily available photodiode equipment. Moreover, we were able to demonstrate a simple way to increase the signal-to-noise ratio for experimental users by reducing the emittance of the unperturbed electron beam. This is a fast and unobtrusive method to improve PPRE performance, albeit operators will have to consider reductions in beam lifetime.

ACKNOWLEDGEMENTS

We wish to thank the I19 beamline staff for their help and cooperation. Seb Wilkes is funded from a joint STFC-Diamond studentship (ST/W507532/1) under supervision by Prof. Philip Burrows.

APPENDIX

Identifying peaks was done via a‘local maxima’ finder in `scipy` [14] which requires as hyperparameters both a threshold for a peak and a minimum distance between peaks. To determine the threshold, we first plotted the fraction of entries larger than a (variable) count size, observing that the photon count distribution followed an exponential decrease with count. To exclude background / noise, we set the peak threshold at the 99.875th percentile of photon counts. Since diffraction peaks are naturally sparse, the minimum distance parameter was less critical. This helped to determine the composition of background. By selecting a signal threshold percentile value of the data, one can subtract off this value across all the data (clamping negative values to zero). We improved the adaptability of this by implementing a $n_b \times n_b$ pixel box around each detected peak. The idea here is help partially tackle signal-induced-noise. We set $n_b \to 25$ and the (local) background threshold to be the 30th percentile.

For the two diffraction measurements, labelled A and B respectively, the cleaned data collected consisted of various peaks times the number of repeats. There is no objective way to average this data, but we believe it makes most physical sense to aggregate the i-the peak's data and then consider the ratio, $R_i = B_i/A_i$. To calculate the final average ratio, $\bar{R} = \text{mean}(\{R_i\})$, a function for performing the average can be specified. The standard arithmetic mean constitutes an unweighted average, and its associated uncertainty comes from quadrature. We also considered weighted arithmetic average, using “inverse-variance weighting”. By selecting this approach, the resulting mean is the maximum likelihood estimator of a system with Gaussian uncertainty [15].

ISBN: 978-3-95450-262-2 ISSN: 2673-5350 doi: 10.18429/JACoW-IBIC2025-TUBC01

REFERENCES

[1] N. L. A. N. Sorgenfrei, E. Giangrisostomi, R. Ovsyannikov, *et al.*, "Photodriven transient picosecond top-layer semiconductor to metal phase-transition in p-doped molybdenum disulfide", *Adv. Mater.*, vol. 33, no. 14, Mar. 2021. doi:10.1002/adma.202006957

[2] C. Kwamen, M. Rössle, W. Leitenberger, *et al.*, "A time-domain perspective on the structural and electronic response in epitaxial ferroelectric thin films on silicon", *Nano Lett.*, vol. 24, no. 31, pp. 9429–9434, Jul. 2024. doi:10.1021/acs.nanolett.4c00712

[3] Diamond Light Source, Machine, 2019, https://www.diamond.ac.uk/Science/Machine.html

[4] *Diamond-II Technical Design Report*, Diamond Light Source, 2023. https://www.diamond.ac.uk/Home/News/LatestNews/2022/14-10-22.html

[5] K. Holldack, R. Ovsyannikov, *et al.*, "Single bunch x-ray pulses on demand from a multi-bunch synchrotron radiation source", *Nat. Commun.*, vol. 5, no. 1, p. 4010, May 2014. doi:10.1038/ncomms5010

[6] G. Rehm, M. G. Abbott, and A. F. D. Morgan, "New features and measurements using the upgraded transverse multibunch feedback at diamond", in *Proc. IBIC'14*, Monterey, CA, USA, Sep. 2014, paper WEPD24, pp. 696–699. https://jacow.org/IBIC2014/papers/WEPD24.pdf

[7] K. Holldack *et al.*, "Two-color synchrotron x-ray spectroscopy based on transverse resonance island buckets", *Sci. Rep.*, vol. 12, no. 1, Sep. 2022. doi:10.1038/s41598-022-19100-z

[8] S. Preston, L. Bobb, AF.D. Morgan, and T. Olsson, "Measurements for emittance feedback based on resonant excitation at diamond light source", in *Proc. IBIC'22*, Kraków, Poland, Sep. 2022, pp. 492–495. doi:10.18429/JACoW-IBIC2022-WEP37

[9] C. Thomas, G. Rehm, I. Martin, and R. Bartolini, "X-ray pinhole camera resolution and emittance measurement", *Phys. Rev. Spec. Top. Accel. Beams*, vol. 13, no. 2, Feb. 2010. doi:10.1103/physrevstab.13.022805

[10] Diamond Light Source, Layout of the I19 beamline, 2025, https://www.diamond.ac.uk/Instruments/Crystallography/I19

[11] S. Wilkes, "Lifetime without compromise", in *Proc. IPAC'23*, Venice, Italy, May 2023, pp. 1068–1070. doi:10.18429/JACoW-IPAC2023-MOPM036

[12] J. Safranek, "Experimental determination of storage ring optics using orbit response measurements", *Nucl. Instrum. Methods Phys. Res. A*, vol. 388, no. 1–2, pp. 27–36, Mar. 1997. doi:10.1016/s0168-9002(97)00309-4

[13] I19 Beamline Staff, Private communication.

[14] SciPy developers, Scipy.signal.find_peaks, 2024, https://docs.scipy.org/doc/scipy/reference/generated/scipy.signal.find_peaks.html

[15] G. Cowan and Particle Data Group, "Estimators for mean, variance, and median", in *Review of Particle Physics*, C. Patrignani *et al.*, Eds. IOP Publishing, 2016, p. 100001. doi:10.1088/1674-1137/40/10/100001